

# Mathematical modeling and simulation of a rectangular pulse transceiver operating in the discrete-time domain

Stevan M. Berber

The University of Auckland,  
Department of Electrical, Computer and Software Engineering,  
Auckland, New Zealand,  
e-mail: s.berber@auckland.ac.nz,  
ORCID ID:  <https://orcid.org/0000-0002-2432-3088>

DOI: 10.5937/vojtehg71-43043; <https://doi.org/10.5937/vojtehg71-43043>

FIELD: electrical engineering, telecommunications

ARTICLE TYPE: original scientific paper

## Abstract:

*Introduction/purpose:* The paper presents the theory and design issues of a discrete-time communication system used for discrete-time pulse transmission with and without filtering. Signals are analyzed in both the time domain and the frequency domain.

*Methods:* The system is theoretically analyzed using block schematics expressed in terms of mathematic operators and the system simulation is performed to confirm the theoretical findings.

*Results:* Discrete-time signals are presented in the time domain and the frequency domain as well as confirmed by a simulation designed in Matlab.

*Conclusion:* The results of the paper contribute to the theoretical modeling and design of modern discrete communication systems.

*Keywords:* discrete communication system, system design, discrete pulse transceiver, filtering, correlation receiver.

## Introduction

Most of the analyses of modern telecommunication systems are based on the presentation of signals in the continuous-time domain, i.e., as continuous functions of time. Consequently, these systems are known under the name of digital communications systems (Haykin, 2001; Proakis, 2001). However, signals of modern communication systems are represented by discrete-time functions and are known under the name of discrete communication systems (Rice, 2009; Berber, 2021; Abramowitz & Stegun, 1972).

This paper aims to present the theoretical base of a discrete communication system assuming that the modulating signal is a

rectangular discrete-time pulse. The content of the paper will include the issues of mathematical modeling and design of a discrete communication system that includes a transmitter, a transmission channel, and a receiver. The signals processed in the system will be presented in the discrete-time domain represented by functions of the discrete-time variable. The system operating in the continuous time domain is named *the digital system*, while the system operating in the discrete-time domain is named *the discrete system* (Miao, 2007; Benvenuto et al, 2007).

Modern designs of transmitters and receivers in a communication system are based on digital technology, primarily on FPGA and DSP platforms. These technologies are in extensive use replacing the analog technologies that are used to implement signal processing functions inside both the baseband and intermediate frequency transceiver blocks. These trends in the design of communication systems became possible due to advances in the theory of discrete-time signal processing, and particularly by the development of the mathematical theory of discrete-time deterministic and stochastic processes (Manolakis et al, 2005; Berber, 2009).

In this paper, all signals inside the transmitter and receiver blocks are analyzed in both the discrete-time domain and the frequency domain. Two different structures of the receiver are analyzed; the first with a low-pass filter and the second with a correlator receiver. To understand the consequences of signal filtering, the transceiver is separately analyzed for the case when a filter is used to reduce the spectrum of the modulating signal, and, consequently, to limit the bandwidth of the modulated signal. The presented system structures are expressed in terms of mathematical operators and their operations are explained using exact mathematical expressions. The designed system is simulated to confirm the theoretical model (Quyen et al, 2015; Ingle & Proakis, 2012).

The related powers and energies of the related signals are precisely calculated for an ideal transmission of signals in the noiseless channel and their filtering. These calculations allowed a clear understanding of the transceiver operation and possible losses in signal power caused by signal processing in the transmitter and receiver blocks.

The theory of discrete-time communication systems is of vital importance for researchers, practicing engineers, and designers of communications devices because the design of these devices is impossible without a deep understanding of the theoretical principles and concepts related to their operation in the discrete-time domain (Rice, 2009; Berber, 2021). Modern communication devices, like wireless and cable modems, TV modems, consumer entertainment systems, and satellite

modems are based on the use of digital processing technology and the principles of the discrete-time signal processing theory.

### Discrete-time communication system structure and operation

A discrete-time communication system, including the basic operation of signals, is presented in Figure 1. The system is composed of a transmitter, a band-pass noise generator, and two types of receivers. The first receiver will demodulate the received band-pass (BP) signal using a low-pass filter (LPF). The second receiver will use a correlator to demodulate the received discrete pulse and generate binary zero (0) or binary one (1) at the output. These two receivers will be separately analyzed. In the case of the system simulation, a band-pass noise generator should be used to generate BP discrete-time noise that will be added to the modulated discrete-time signal. The BP noise generation and application for the system investigation is a separate topic.

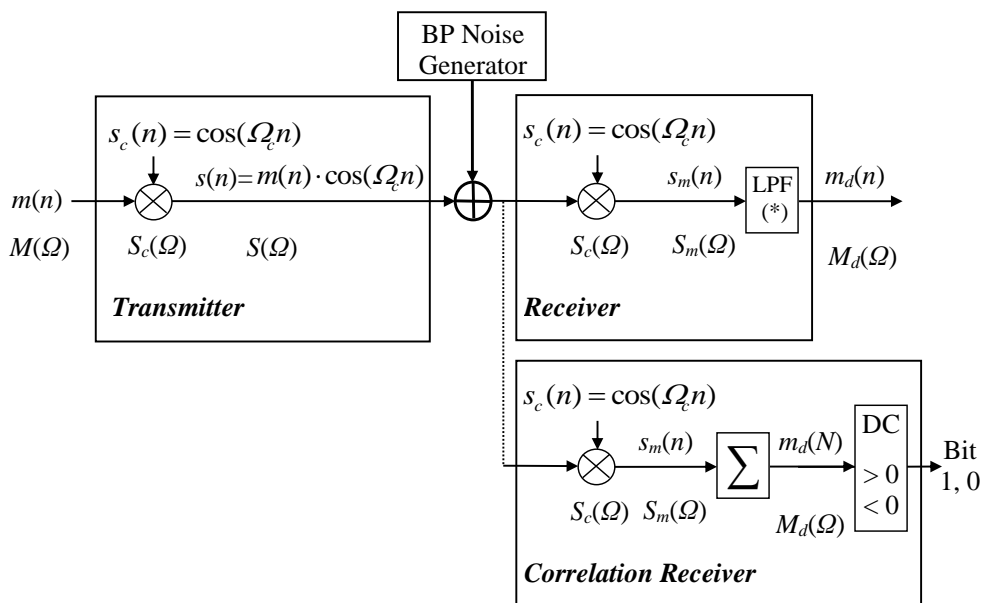


Figure 1 – Discrete communication system  
 Рис. 1 – Дискретная система связи  
 Слика 1 – Дискретни телекомуникациони систем

## Transmitter operation

Suppose the output of the transmitter is a product of a modulating discrete-time (dt) rectangular pulse  $m(n)$  and the discrete-time carrier  $s_c(n) = \cos \Omega_c n$  resulting in a dt modulated signal  $s(n)$ , expressed in this form

$$s(n) = m(n) \cos \Omega_c n, \quad (1)$$

as shown in Figure 1. We are to find the expression in the time domain and in the frequency domain of the modulated signal and all signals involved in signal processing, assuming that the dt rectangular pulse is of an amplitude  $A$  and a duration  $N$  while the frequency of the carrier is  $\Omega_c$ .

*The rectangular pulse in the time domain and the frequency domain.* The graphs of the dt rectangular pulse in the discrete-time domain are presented in Figure 2. The rectangular pulse in the time domain can be expressed in terms of Koronecker's delta function as a convolution of the signal and the delta functions, i.e.,

$$m(n) = \begin{cases} A & 0 \leq n \leq N-1 \\ 0 & \text{otherwise} \end{cases} = \sum_{k=-\infty}^{\infty} m(k) \delta(n-k) = \sum_{k=0}^{N-1} m(k) \delta(n-k) \quad (2)$$

for its amplitude  $A = 2$  and duration  $N = 8$  as shown in Figure 2. The pulse values are defined for each whole number  $n$  and have no values in the intervals between neighboring numbers. We can say that the signal does not exist in these intervals. The intervals are used to process the discrete signal values.

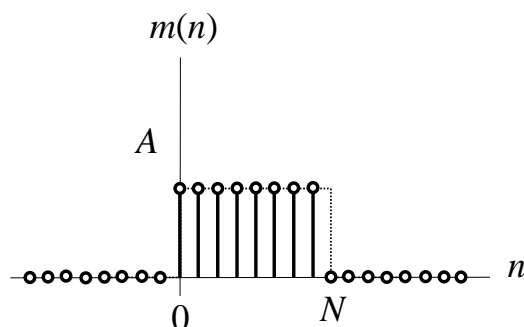


Figure 2 – Discrete-time modulating signal for  $N = 8$  and  $A = 2$ .

Рис. 2 – Модулирующий сигнал с дискретным временем для  $N = 8$  и  $A = 2$

Слика 2 – Модулушући сигнал дискретног времена за  $N = 8$  и  $A = 2$

To find the amplitude and magnitude spectral densities of the pulse, we need to find the discrete-time Fourier transform (DTFT) of the modulating signal which is a discrete-time rectangular pulse. Based on the property of Kronecker's delta function, the DTFT of the dt pulse that has  $A$  values in the interval from 0 to  $(N-1)$  can be expressed in the following form (Berber, 2021)

$$\begin{aligned}
 M(\Omega) &= \sum_{n=-\infty}^{\infty} m(n)e^{-j\Omega n} = \sum_{n=-\infty}^{\infty} \sum_{k=0}^{N-1} m(k)\delta(n-k)e^{-j\Omega n} \\
 &= \sum_{k=0}^{N-1} m(k) \sum_{n=-\infty}^{\infty} \delta(n-k)e^{-j\Omega n} = \sum_{k=0}^{N-1} Ae^{-j\Omega k} = \sum_{k=n}^{n=(N-1)} Ae^{-j\Omega n} \quad (3)
 \end{aligned}$$

Then, the amplitude spectral density can be calculated as

$$\begin{aligned}
 M(\Omega) &= \sum_{k=0}^{N-1} Ae^{-j\Omega k} = \sum_{k=n}^{n=(N-1)} Ae^{-j\Omega n} = A \frac{1-e^{-j\Omega N}}{1-e^{-j\Omega}} = Ae^{-j\Omega(N-1)/2} \frac{\sin(\Omega N/2)}{\sin(\Omega/2)} \\
 &= \left\{ \begin{array}{ll} AN & \Omega = \pm 2k\pi, k = 0, 1, 2, 3, \dots \\ Ae^{-j\Omega(N-1)/2} \frac{\sin(\Omega N/2)}{\sin(\Omega/2)} & otherwise \end{array} \right\} \quad (4)
 \end{aligned}$$

Having the amplitude spectral density, we can calculate the magnitude spectral density expressed as

$$|M(\Omega)| = \left\{ \begin{array}{ll} AN & \Omega = \pm 2k\pi, k = 0, 1, 2, 3, \dots \\ A \left| \frac{\sin(\Omega N/2)}{\sin(\Omega/2)} \right| & otherwise \end{array} \right\}, \quad (5)$$

and the phase spectral density is expressed as

$$\arg M(\Omega) = -\frac{\Omega}{2}(N-1) + \arg \frac{\sin(\Omega N/2)}{\sin(\Omega/2)}, \quad (6)$$

which are presented in Figure 3 for the case of  $N = 8$  and  $A = 2$ . Note that the amplitude value of  $M(\Omega)$  for  $\Omega = 0$  is equal to  $AN$ , which can be easily obtained by calculating this value from the defining expression for the DTFT. The magnitude spectral density  $M(\Omega)$  is a periodic function with a period of  $2\pi$ . The zeros crossings in this function occur for the condition  $\sin(\Omega_0 N/2) = 0$ , i.e., for  $\Omega_0 N/2 = k\pi$ ,  $k = 1, 2, \dots, N-1$ . For  $N = 8$ , we may have  $\Omega_0 = \pm 2k\pi/N = \pm k\pi/4$ , and  $k = 1, 2, \dots, N-1$ . The phase discontinuities of  $\pi$  radians occur at the same frequencies.

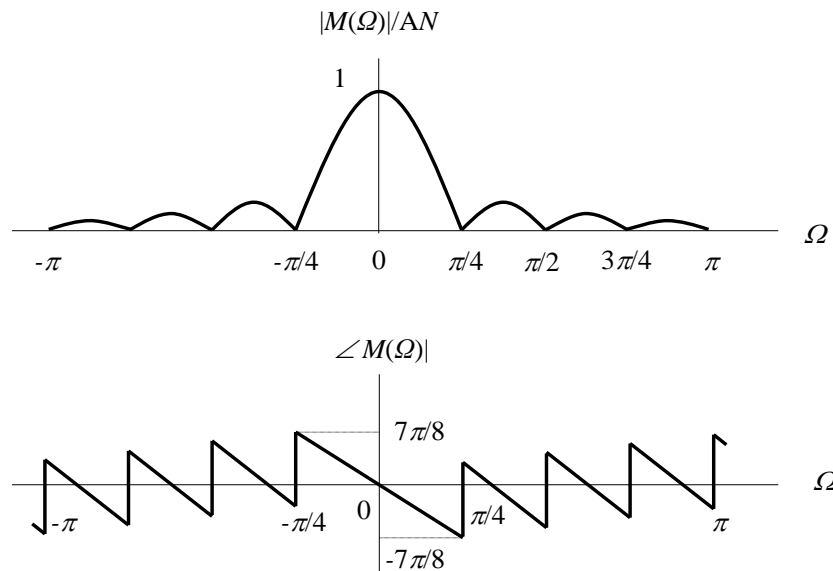


Figure 3 – Magnitude and phase spectral densities of the modulating signal  
 Рис. 3 – Спектральная плотность колебаний и фазы модулирующего сигнала  
 Слика 3 – Спектрална густина магнитуде и фазе модулишућег сигнала

The power and energy of the pulse can be calculated in the time domain and in the frequency domain. In the time domain, the power is

$$P_m = \frac{1}{N} \sum_{n=0}^{N-1} m^2(n) = \frac{1}{8} \sum_{n=0}^{n=7} A^2 = A^2, \quad (7)$$

and the related energy is calculated as

$$E_m = P_m \cdot N = \sum_{n=0}^{N-1} m^2(n) = \sum_{n=0}^{n=7} A^2 = 8A^2. \quad (8)$$

The modulating signal  $m(n)$  is an energy signal. Therefore, its energy spectral density can be calculated as

$$E_m(\Omega) = |M(\Omega)|^2 = A^2 \left| \frac{\sin(\Omega N / 2)}{\sin(\Omega / 2)} \right|^2. \quad (9)$$

This function can be calculated as the DTFT of its autocorrelation function (Berber, 2019). The energy is the integral of the energy spectral density calculated as (Integral calculator, 2023)

$$E_m = \frac{1}{2\pi} \int_{-\pi}^{\pi} E_m(\Omega) d\Omega = \frac{A^2}{2\pi} \int_{-\pi}^{\pi} \left| \frac{\sin(4\Omega)}{\sin(\Omega / 2)} \right|^2 d\Omega = \frac{A^2}{2\pi} 16\pi = 8A^2, \quad (10)$$

and the power of the pulse is

$$P_m = \frac{E_m}{N} = A^2. \quad (11)$$

The energy inside the first arcade (Figure 3) can be calculated as

$$E_{m1} = \frac{A^2}{2\pi} \int_{-\pi/4}^{\pi/4} \left| \frac{\sin 4\Omega}{\sin(\Omega/2)} \right|^2 d\Omega = \frac{A^2}{2\pi} 45.64495506949089, \quad (12)$$

and the energy inside both the first and second arcades is

$$E_{m1-2} = \frac{A^2}{2\pi} \int_{-\pi/2}^{\pi/2} \left| \frac{\sin 4\Omega}{\sin(\Omega/2)} \right|^2 d\Omega = \frac{A^2}{2\pi} 48.29464599062311, \quad (13)$$

which corresponds to 90.81% and 96.08% of the total signal energy, respectively. Therefore, if we are filtering the first arcade of the signal, we will use only 90.81% of the signal power.

*Discrete-time carrier in the time domain and the frequency domain.* Suppose the discrete-time carrier has a unit amplitude, i.e., it is expressed as  $s_c(n) = \cos \Omega_c n$ . Suppose the carrier has only  $N_c = 4$  samples per oscillation. Therefore, we can calculate its frequency  $\Omega_c = 2\pi f_c / f_s = 2\pi / N_c = \pi / 2$ , and express it in the discrete-time domain as

$$s_c(n) = \cos \Omega_c n = \cos 2\pi n / N_c = \cos \pi n / 2, \quad (14)$$

which is shown in the graphical form in Figure 4. The carrier in the frequency domain can be directly found for any  $N_c$  simply applying Euler's formula on the time domain signal as

$$s_c(n) = \frac{1}{2} [e^{j\Omega_c n} + e^{-j\Omega_c n}] = \frac{1}{2} [e^{j2\pi n/N_c} + e^{-j2\pi n/N_c}] = \frac{1}{2} [e^{j2\pi n/N_c} + e^{j2\pi n(N_c-1)/N_c}].$$

For the case analyzed  $N_c = 4$  and  $\Omega_c = \pi / 2$ , we may express the carrier in the time domain as

$$s_c(n) = \frac{1}{2} [e^{j\pi n/2} + e^{j\pi n3/2}], \quad (15)$$

and in the frequency domain as

$$S_c(\Omega) = \sum_{k=\pm 1} \frac{2\pi}{2} \delta(\Omega + k \cdot \Omega_c) = \pi \delta(\Omega + \Omega_c) + \pi \delta(\Omega - \Omega_c). \quad (16)$$

Because this signal is a periodic function of the continuous frequency  $\Omega$  with a period of  $2\pi$ , it can be represented by a periodic stream of Dirac's delta functions (Papoulis & Pillai, 2002), as presented in Figure 4.

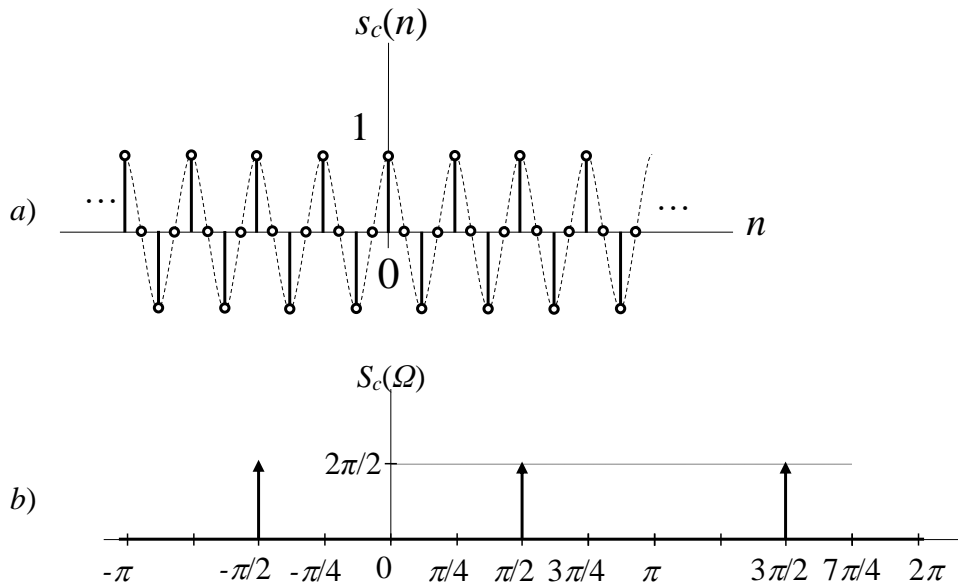


Figure 4 – a) Waveshape of the carrier, b) related amplitude spectral density  
 Рис. 4 – а) Форма несущей волны, б) относительная спектральная плотность колебаний  
 Слика 4 – а) Таласни облик носиоца, б) односна спектрална густина амплитуде

Based on (14), the power of the carrier can be calculated in the time domain as

$$P_c = \frac{1}{4} \sum_{n=0}^{n=3} \cos^2(\pi n / 2) = \frac{1}{4} \sum_{n=0}^{n=3} \frac{1}{2} (1 + \cos \pi n) = \frac{1}{4} \sum_{n=0}^{n=3} \frac{1}{2} = \frac{1}{2}. \quad (17)$$

The carrier is a power signal (Cavicchi, 2000; Berber, 2021). Therefore, its average power is to be calculated in an infinite interval, according to this expression

$$P_c = \lim_{a \rightarrow \infty} \frac{1}{2a} \sum_{n=-a}^a \cos^2(\Omega_c n) = \lim_{a \rightarrow \infty} \frac{1}{2a} \sum_{n=-a}^a \frac{1}{2} (1 + \cos \pi n) = \lim_{a \rightarrow \infty} \frac{1}{2a} \frac{2a}{2} = \frac{1}{2}, \quad (18)$$

resulting in the same value as in (17). Because the carrier is a power signal, its energy is expected to be infinite. We can confirm that by calculating the energy of the signal in the frequency domain as



$$\begin{aligned}
 E_c &= \frac{1}{2\pi} \int_{-\infty}^{\infty} |S_c^2(\Omega)| d\Omega = \frac{1}{2\pi} \int_{-\infty}^{\infty} \left( \sum_{k=\pm 1} \frac{2\pi}{2} \delta(\Omega + k\Omega_c) \right)^2 d\Omega \\
 &= \frac{\pi}{2} \int_{-\infty}^{\infty} \left( \delta^2(\Omega + \Omega_c) + 2\delta(\Omega + \Omega_c)\delta(\Omega - \Omega_c) + \delta^2(\Omega - \Omega_c) \right) d\Omega \\
 &= \frac{\pi}{2} \int_{-\infty}^{\infty} \delta(\Omega + \Omega_c)\delta(\Omega + \Omega_c) d\Omega + 0 + \frac{\pi}{2} \int_{-\infty}^{\infty} \delta(\Omega - \Omega_c)\delta(\Omega - \Omega_c) d\Omega \\
 &= \frac{\pi}{2} (\delta(-\Omega_c + \Omega_c) + \delta(\Omega_c - \Omega_c)) = \pi\delta(0) = \infty
 \end{aligned} \tag{19}$$

because the integral of the product of the two delta functions is zero and the integral of the delta function squared can be considered infinity. The infinite energy value can be confirmed by its calculation in the time domain as

$$E_c = \lim_{a \rightarrow \infty} \sum_{n=-a}^a \cos^2(\Omega_c n) = \lim_{a \rightarrow \infty} \sum_{n=-a}^a \frac{1}{2} (1 + \cos \pi n) = \lim_{a \rightarrow \infty} \frac{2a}{2} = \infty. \tag{20}$$

### Modulated signal in the time domain and the frequency domain

Plot the graphs of all signals in the frequency domain assuming that the number of samples of the rectangular pulse is  $N = 8$  and there are two oscillations of the carrier inside the pulse, i.e., one oscillation of the carrier is represented by  $N_c = 4$  samples. The rectangular pulse in the discrete-time domain has already been expressed by (2). With a precise definition of the modulating signal  $m(n)$  in the time domain, the modulated signal can be expressed in terms of Kronecker delta functions as

$$\begin{aligned}
 s(n) &= m(n) \cos \Omega_c n = \cos \Omega_c n \sum_{k=0}^{N-1} m(k) \delta(n-k) = \sum_{k=0}^{N-1} m(k) \delta(n-k) \cos \Omega_c n \\
 &= A \sum_{k=0}^{N-1} \delta(n-k) \cos \Omega_c n
 \end{aligned} \tag{21}$$

and graphically presented as in Figure 5. We may get the amplitude spectral density of that signal as the convolution of the modulating signal and the carrier in the frequency domain (Berber, 2021), which will give the modulated signal as

$$\begin{aligned}
 S(\Omega) &= M(\Omega) * S_c(\Omega) = \frac{1}{2\pi} \int_{-\infty}^{\infty} M(\lambda) \cdot S_c(\Omega - \lambda) d\lambda = \\
 &= \frac{1}{2\pi} \int_{-\infty}^{\infty} M(\lambda) \cdot \frac{2\pi}{2} \delta(\Omega + \Omega_c - \lambda) d\lambda + \frac{1}{2\pi} \int_{-\infty}^{\infty} M(\lambda) \cdot \frac{2\pi}{2} \delta(\Omega - \Omega_c - \lambda) d\lambda \cdot (22) \\
 &= \frac{1}{2} M(\Omega + \Omega_c) + \frac{1}{2} M(\Omega - \Omega_c)
 \end{aligned}$$

Based on the expression for the amplitude spectral density of  $m(n)$  (5), the required frequency-shifted components in (22) can be expressed as

$$\begin{aligned}
 \frac{1}{2} M(\Omega \pm \Omega_c) &= \frac{A}{2} e^{-j(\Omega \pm \Omega_c)(N-1)/2} \frac{\sin((\Omega \pm \Omega_c)N/2)}{\sin((\Omega \pm \Omega_c)/2)} \\
 &= \left\{ \begin{array}{ll} AN/2 & \Omega \pm \Omega_c = \pm 2k\pi, k = 0, 1, 2, 3, \dots \\ \frac{A}{2} e^{-j(\Omega \pm \Omega_c)(N-1)/2} \frac{\sin((\Omega \pm \Omega_c)N/2)}{\sin((\Omega \pm \Omega_c)/2)} & \text{otherwise} \end{array} \right\} \cdot (23)
 \end{aligned}$$

The magnitude spectral density of the modulated signal is presented in Figure 5.

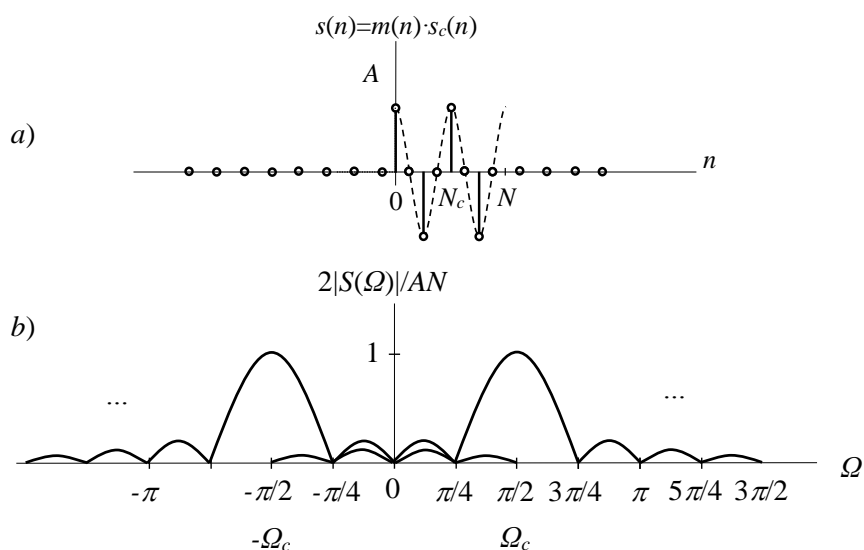


Figure 5 – a) Discrete-time waveshape, and b) magnitude spectral density of the modulated signal

Рис. 5 – а) Форма волны с дискретным временем и б) спектральная плотность модулированного сигнала по величине

Слика 5 – а) Таласни облик у дискретном времену, б) спектрална густина магнитуде модулисаног сигнала

The magnitude spectrum is a periodic function with a period of  $2\pi$ . The two-sided spectrum of the signal can be investigated inside the bandwidth around the carrier frequency of  $\pi/2$ . We can calculate the signal energy and power in the time domain

$$E_s = P_s \cdot N = \sum_{n=0}^{N-1} s^2(n) = \sum_{n=0}^{n=7} s^2(n) = 4A^2 \quad (24)$$

and the power is

$$P_s = E_s / N = 4A^2 / 8 = A^2 / 2. \quad (25)$$

The energy calculated in the frequency domain confirms calculations in the time domain, i.e.,

$$\begin{aligned} E_s &= \frac{1}{2\pi} \int_{-\pi}^{\pi} |S(\Omega)|^2 d\Omega = \frac{1}{2\pi} \int_{-\pi}^{\pi} \left| \frac{1}{2} [M(\Omega - \Omega_c) + M(\Omega + \Omega_c)] \right|^2 d\Omega \\ &= \frac{1}{\pi} \frac{A^2}{4} \int_{-\pi}^{\pi} |M(\Omega - \Omega_c)|^2 d\Omega = \frac{A^2}{4\pi} \int_{-\pi}^{\pi} \left| \frac{\sin((\Omega \pm \Omega_c)4)}{\sin((\Omega \pm \Omega_c)/2)} \right|^2 d\Omega = \frac{A^2}{4\pi} 16\pi = 4A^2 \end{aligned} \quad (26)$$

The modulated signal is an energy signal having finite energy. The power calculated in the signal interval is finite.

However, if the average power is calculated in the infinite interval, it would be of zero value which complies with the definition of the power signals.

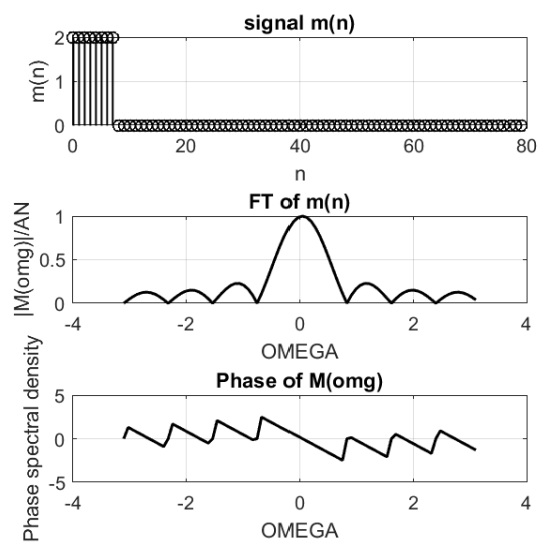
### Simulation of the transmitter operation

We performed a simulation of the transmitter presented in Figure 1 (Ingle & Proakis, 2012).

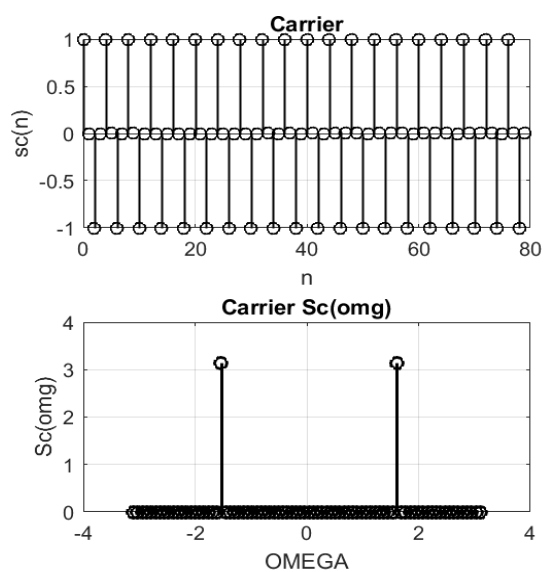
The signals are generated in the time domain and the frequency domain.

The modulating signal and the carrier obtained by simulation in the time domain and the frequency domain are presented in Figure 6.

They are equivalent to the signals obtained by calculations and presented in Figures 3 and 4, respectively.



a)



b)

Figure 6 – Magnitude and phase spectra: a) the modulating signal, b) the carrier  
 Рис. 6 – Амплитудный и фазовый спектры: а) модулирующего сигнала, б) несущей волны

Слика 6 – Спектри магнитуде и фазе: а) модулишући сигнал, б) носилац

A simulated modulated signal in the time domain and the frequency domain is presented in Figure 7. The presentations are equivalent to the graphs obtained by calculations and shown in Figure 5.

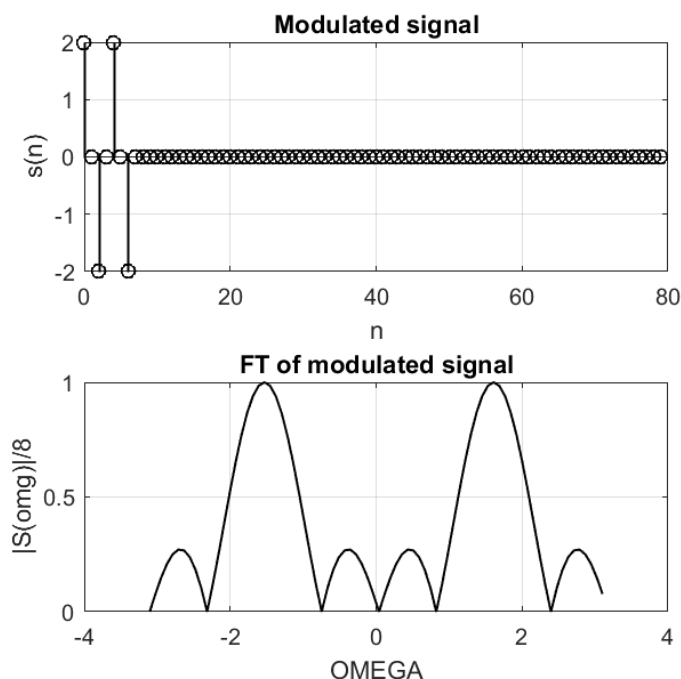


Figure 7 – Magnitude spectral density of the modulated signal in the time domain and in the frequency domain

Рис. 7 – Спектральная плотность колебаний модулированного сигнала во временной и частотной областях

Слика 7 – Спектрална густина магнитуде модулисаног сигнала у временској и фреквенцијској домени

### Receiver operation with the implementation of a low-pass filter

The demodulation of the discrete modulate signal results in the discovery of a modulating signal that is in the form of a rectangular pulse. The procedure of demodulation takes place inside the receiver as presented in Figure 1. We will first analyze the case when a low-pass filter is used to demodulate the modulated signal. We use a coherent receiver in this case. Firstly, the received signal is multiplied by the carrier to get the multiplied signal

$$s_m(n) = m(n) \cos^2 \Omega_c n = \begin{cases} \frac{1}{2} A(1 + \cos 2\Omega_c n) & 0 \leq n \leq N-1 \\ 0 & \text{otherwise} \end{cases}. \quad (27)$$

The wave shape of this signal is shown in Figure 8. The signal is represented by 4 discrete amplitude  $A$  values. The dashed graph notifies what the shape of the corresponding continuous-time signal would look like. The DC component of the signal having amplitude  $A/2$  is also presented in Figure 8. The double frequency term of the discrete time signal is  $\cos 2\Omega_c n = \cos 4\pi n / N_c = \cos 4\pi n / 4 = \cos \pi n$ .

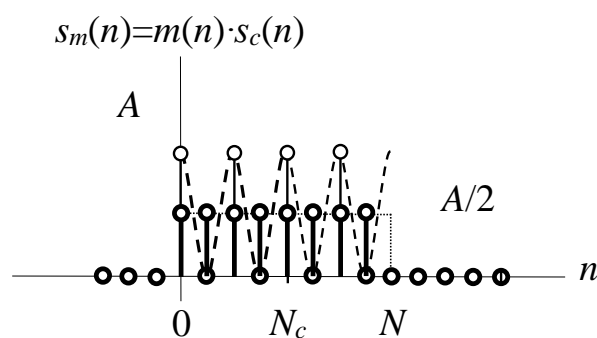


Figure 8 - The output of the signal multiplier  
 Рис. 8 - Выходной сигнал умножителя сигнала  
 Слика 8 - Излаз множача сигнала

The DTFT of this signal gives its amplitude spectral density of the form

$$\begin{aligned} S_m(\Omega) &= \frac{1}{2} FT \{m(n)(1 + \cos 2\Omega_c n)\} = \frac{1}{2} FT \{m(n) + m(n) \cos 2\Omega_c n\} \\ &= \frac{1}{2} M(\Omega) + \frac{1}{4} [M(\Omega - 2\Omega_c) + M(\Omega + 2\Omega_c)] \end{aligned}, \quad (28)$$

where the amplitude spectral density of the low-frequency part is

$$\frac{1}{2} M(\Omega) = \begin{cases} AN/2 & \Omega = \pm 2k\pi, k = 0, 1, 2, 3, \dots \\ \frac{A}{2} e^{-j\Omega(N-1)/2} \frac{\sin(\Omega N/2)}{\sin(\Omega/2)} & \text{otherwise} \end{cases}. \quad (29)$$

The amplitude spectral density of the LF signal part is shown in Figure 9. This spectrum has the same wavelshape as the spectrum of the modulating signal in Figure 3, but all of its amplitudes are two times smaller due to the processing inside the demodulator.

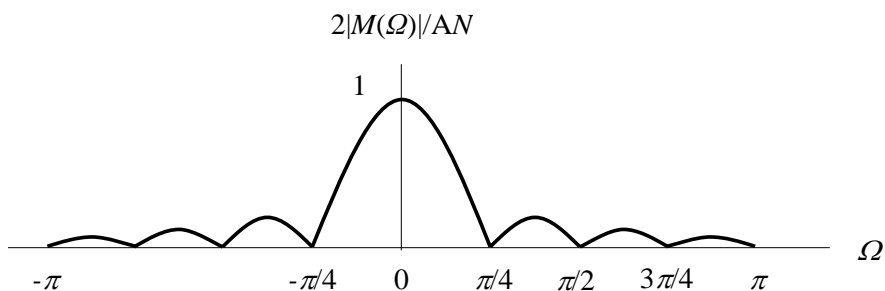


Figure 9 – Magnitude spectral density of the demodulated pulse  
 Рис. 9 – Амплитудная спектральная плотность демодулированного импульса  
 Слика 9 – Спектрална густина магнитуде демодулисаног пулса

Also, the shifted components of the signal are

$$\frac{1}{4} M(\Omega \pm 2\Omega_c) = \frac{A}{4} e^{-j(\Omega \pm 2\Omega_c)(N-1)/2} \frac{\sin((\Omega \pm 2\Omega_c)N/2)}{\sin((\Omega \pm 2\Omega_c)/2)}$$

$$= \left\{ \begin{array}{ll} AN/4 & \Omega \pm 2\Omega_c = \pm 2k\pi, k=0, 1, 2, 3, \dots \\ \frac{A}{4} e^{-j(\Omega \pm 2\Omega_c)(N-1)/2} \frac{\sin((\Omega \pm 2\Omega_c)N/2)}{\sin((\Omega \pm 2\Omega_c)/2)} & \text{otherwise} \end{array} \right\}, (30)$$

and the spectrum of the signal at the output of the multiplier is presented in Figure 10.

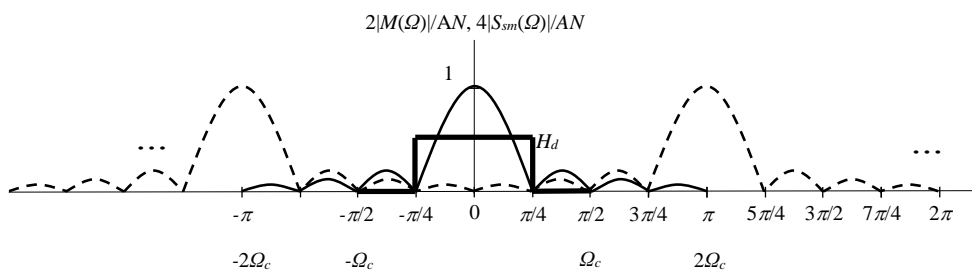


Figure 10 – The spectrum of the signal at the output of the multiplier  
 Рис. 10 – Спектр сигнала на выходе умножителя  
 Слика 10 – Спектар сигнала на излазу множача

The power and energy of the demodulated signal can be calculated in both the time domain and the frequency domain. With expression (27), the energy calculated in the time domain can be calculated as

$$\begin{aligned}
 E_{sm} &= \sum_{n=0}^{n=7} \left( \frac{1}{2} A(1 + \cos 2\Omega_c n) \right)^2 = \sum_{n=0}^{n=7} \frac{1}{4} A^2 + \frac{1}{4} \sum_{n=0}^{n=7} A^2 \left( \frac{1}{2} + \frac{1}{2} \cos 4\Omega_c n \right) \\
 &= \sum_{n=0}^{n=7} \frac{1}{4} A^2 + \frac{1}{8} \sum_{n=0}^{n=7} A^2 = 3A^2
 \end{aligned} \tag{31}$$

and the power is

$$P_{sm} = \frac{E_{sm}}{N} = \frac{3A^2}{8} . \tag{32}$$

Using the magnitude spectral density (28), we can find the energy spectral density. Then, the energy is calculated as the integral value of the energy spectral density, i.e.,

$$\begin{aligned}
 E_{sm} &= \frac{1}{2\pi} \int_{-\pi}^{\pi} \left| \frac{1}{2} M(\Omega_c) + \frac{1}{4} M(\Omega - 2\Omega_c) + \frac{1}{4} M(\Omega + 2\Omega_c) \right|^2 d\Omega \\
 &= \left( 2 + \frac{1}{4} \right) A^2 = 3A^2
 \end{aligned} , \tag{33}$$

which also confirms the value of the signal power expressed in (32).

*LPF operation in time and frequency domain.* If the LP filter with the cut-off frequency  $\Omega_F = \pi/4$  and the gain  $H_d$  is used to eliminate the HF components at the double carrier frequency, as shown in Figure 10, the demodulated pulse at the output of the LPF, as shown in Figure 1, can be obtained and expressed in the frequency domain as

$$M_d(\Omega) = S_m(\Omega)H_d(\Omega) \approx \begin{cases} H_d \cdot M(\Omega)/2 & |\Omega| \leq \Omega_F = \pi/4 \\ 0 & \text{otherwise} \end{cases} . \tag{34}$$

We also assume that the double carrier frequency components in the LP filter bandwidth are negligibly small. We intend to find the signal at the output of the LPF in the time domain. For that purpose, we can perform a convolution of the LPF input signal and the impulse response of the filter. Therefore, we need to calculate first the impulse response of the filter  $h(n)$ . The LPF here is considered an LTI system. Then, the impulse response of the filter is the DTFT of the filter impulse response, i.e.,



$$h(n) = \frac{1}{2\pi} \int_{-\pi}^{\pi} H_d(\Omega) e^{j\Omega n} d\Omega = \frac{1}{2\pi} \int_{-\Omega_F}^{\Omega_F} H_d e^{j\Omega n} d\Omega = \frac{H_d \Omega_F}{\pi} \text{sinc} \Omega_F n$$

$$= \frac{H_d}{\Omega_F = \pi/4} \text{sinc} \pi n / 4 \quad , \quad (35)$$

for the assumed cut-off frequency of the LP filter of  $\Omega_F = \pi/4$ , as shown in Figure 10. The zero crossings are calculated as:  $\sin(\pi n / 2) = 0$ ,  $(\pi n / 2) = k\pi$ , and  $n = 2k$ . The demodulated pulse in the time domain can be obtained as the convolution of the input signal  $s_m(n)$  and the impulse response  $h(n)$ , i.e.,

$$m_d(n) = \sum_{l=-\infty}^{l=\infty} h(n-l) s_m(l) = \sum_{l=-\infty}^{l=\infty} s_m(n-l) h(l) = \sum_{l=n-(N-1)}^{l=n} s_m(n-l) h(l) \quad . \quad (36)$$

The procedure of doing the convolution is presented in Figure 11. For a fixed position of the demodulated signal on the  $n$ -axis, the time-inverted impulse response is shifted from minus infinity to plus infinity, and the corresponding products are added for every  $n$  value, as notified in Figure 11.

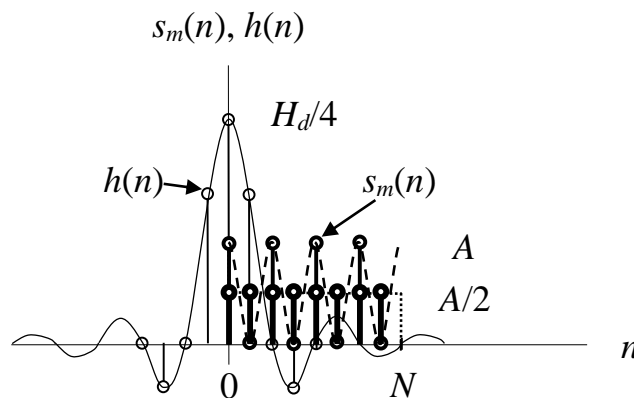


Figure 11 - Convolution of the signals  
 Рис. 11 - Свертка сигналов  
 Слика 11 - Конволуција сигнала

The energy of the received rectangular pulse is expressed as (34),

$$E_{md}(\Omega) = |M(\Omega)|^2 = |H_d \cdot M(\Omega) / 2|^2 = \frac{H_d^2}{4} |M(\Omega)|^2 = \frac{H_d^2}{4} A^2 \left| \frac{\sin(\Omega N / 2)}{\sin(\Omega / 2)} \right|^2 \quad . \quad (37)$$

The energy is the integral of the energy spectral density calculated as

$$E_{md} = \frac{1}{2\pi} \int_{-\pi}^{\pi} E_{md}(\Omega) d\Omega = \frac{H_d^2 A^2}{4} \int_{-\pi}^{\pi} \left| \frac{\sin 4\Omega}{\sin(\Omega/2)} \right|^2 d\Omega = \frac{H_d^2}{4} E_m = 2H_d^2 A^2, \quad (38)$$

and the power of the pulse is

$$P_{md} = \frac{E_{md}}{N} = \frac{H_d^2 E_m}{4 N} = \frac{H_d^2}{4} P_m. \quad (39)$$

Comparing relation (39) with expression (11), we can see that the power of the modulating signal at the transmitter side is attenuated  $H_d^2 / 4$  times. If we assume that the filter is defined by  $H_d = 1$ , the power will be attenuated 4 times, or 6.02 dB as it can be seen from this simple calculation.

$$a = 10 \log_{10}(P_{md} / P_m) = 10 \log_{10}(4 / H_d^2) = 10 \log_{10} 4 = 6.02 \text{ dB}. \quad (40)$$

In a real system, we will have additional attenuation of the signal due to the propagation and the influence of noise and fading, which will further complicate the procedures of signal processing inside both the transmitter and the receiver.

### Simulation of the receiver

We performed a simulation of the receiver presented in Figure 1.

The signals are generated in the time domain and the frequency domain. The demodulated signal obtained by simulation in the time domain and the frequency domain is presented in Figure 12.

The waveshapes of this signal are equivalent to the signals obtained by calculations and presented in Figure 8 and Figure 10.

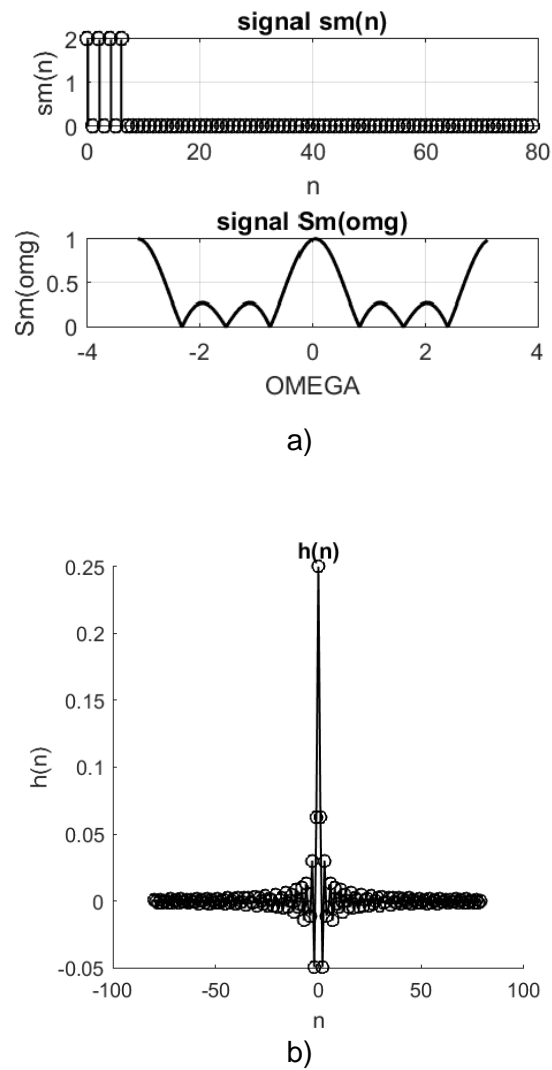
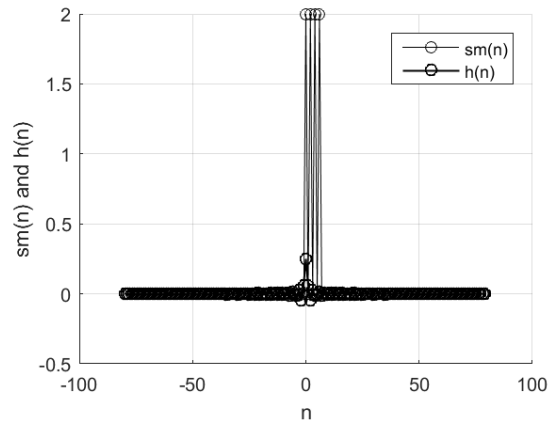


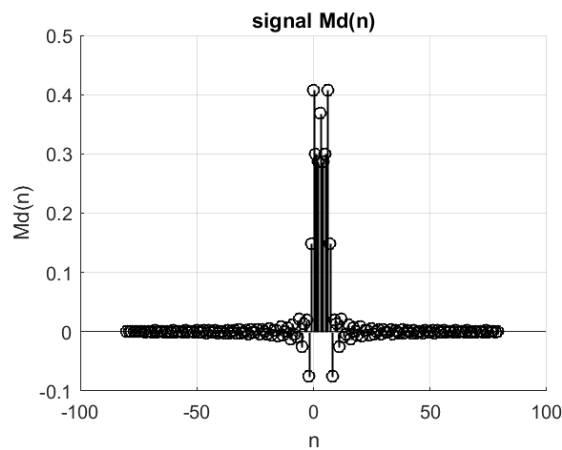
Figure 12 – a) The demodulated signal, b) the impulse response of the LP filter for  $N = 8$ ,  $\Omega_F = \pi / 4$  and  $H_d = 1$

Рис. 12 – а) Демодулированный сигнал, б) импульсная характеристика LP-фильтра для  $N = 8$ ,  $\Omega_F = \pi / 4$  и  $H_d = 1$

Слика 12 – а) Демодулисани сигнал, б) импулсни одзив нископропусног филтера за  $N = 8$ ,  $\Omega_F = \pi / 4$  и  $H_d = 1$



a)



b)

Figure 13 – a) Convolution procedure of the demodulated signal and the impulse response, b) the output signal obtained by convolution

Рис. 13 – а) Процедура свертки демодулированного сигнала и импульсного отклика, б) выходной сигнал, полученный путем свертки

Слика 13 – а) Поступак конволуције демодулисаног сигнала и импулсног одзива, б) излазни сигнал након конволуције

The impulse response of the LP filter is presented in Figure 12b). The procedure of the correlation is presented in Figure 13a) while the waveshape of the LP filter output is presented in Figure 13b).

## Correlation receiver implementation and operation

As we have seen, the demodulation of the discrete modulated signal using the LPF results in the discovery of the modulating signal that is in a form of a rectangular pulse. Based on the sign of the pulse received, the Decision Circuit decides on the binary value of the transmitted signal. For the positive pulse, it is said that 1 was transmitted and for the negative pulse, it is said that 0 was transmitted.

For the same structure of the transmitter, the procedure of demodulation takes place inside the correlation receiver as presented in Figure 1 (lower block on the right). The received signal is first multiplied by the carrier to get the signal  $s_m(n)$  as in (27). This signal in the frequency domain is given by expression (28). The wave shape of this signal is shown in Figure 8. The samples of the signal are accumulated inside the correlator adder to get

$$m_d(N) = \sum_{n=0}^{N-1} s_m(n) = \sum_{n=0}^{N-1} \frac{1}{2} A(1 + \cos 2\Omega_c n) = \sum_{n=0}^{N-1} \frac{1}{2} A + \sum_{n=0}^{N-1} \cos 2\Omega_c n = \frac{1}{2} AN. \quad (41)$$

The Decision Circuit decides on the  $m_d(N)$  value and generates, at its output, 1 or 0 according to this decision rule

$$DC_{out} = \begin{cases} 1 & m_d(N) \geq 0 \\ 0 & m_d(N) < 0 \end{cases}. \quad (42)$$

If we send a stream of bits 1 and 0 (by changing the sense of the amplitude  $A$  inside  $m(n)$ ) at the transmitter side, the receiver will generate the same stream at its output. Each bit will be generated at the time instants  $iN$ , where  $i$  is a set of natural numbers and  $N$  is the number of samplers in each discrete pulse  $m(n)$ . This is the case when noise is not present in the channel, i.e., the channel is noiseless. Therefore, in the system with a noiseless channel, the decision will always be correct in the Decision Circuit. Namely, if a positive pulse is transferred, meaning that the amplitude  $A$  is positive, the product (41) will be positive and the Decision Circuit will generate bit 1 (one) at the output. If a negative pulse is transmitted, the product (41) will be negative and the Decision Circuit will generate bit 0 (zero) at the output. We design transceiver blocks and use the noiseless channel to investigate the operation of the transceiver blocks only. When we are sure the blocks are operating properly, we add the channel simulator to investigate the properties of the whole system in real conditions. In the presence of noise, the sign of the product (41) can be changed due to the noise level and the wrong decision can be made.

## Discrete communication system for the transmission of a filtered pulse

To reduce interference between communication systems, we can use filtering inside the transmitter. That filtering limits the spectrum of the transmitted signal. We will analyze the case when the modulating signal is filtered by an LPF and then transmitted through the transmitter circuits and received by the receiver circuits in the same way as explained in the previous sections. The block scheme of the transmitter with the LP filter is presented in Figure 14.

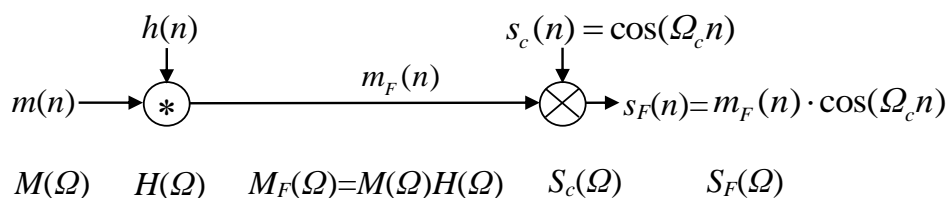


*Figure 14 – Discrete-filtered pulse modulator*  
*Рис. 14 – Импульсный модулятор с дискретной фильтрацией*  
*Слика 14 – Модулятор дискретног и филтрираног пулса*

At the input of the transmitter, there is a discrete rectangular pulse as in the previously analyzed transmitter. The pulse is already presented in the time domain and the frequency domain in the previous sections. At the output of the transmitter, there is the modulated signal  $s_F(n)$  that corresponds to the modulated signal  $s(n)$  in Figure 1.

*The LP Filter operation.* To limit the bandwidth of the signal, we will use an LPF of the gain  $H$ , which will filter out the first two arcades of the rectangular pulse defined by the cut-off frequency  $\Omega_F$ , as shown in Figure 15. In this case, we will limit the power of the filtered pulse to 96.08 % of the pulse total power as calculated in (13). The filter transfer characteristic in the frequency domain is defined as

$$H(\Omega) = \begin{cases} H & |\Omega| \leq \Omega_F = \pi / 2 \\ 0 & \text{otherwise} \end{cases}. \quad (43)$$

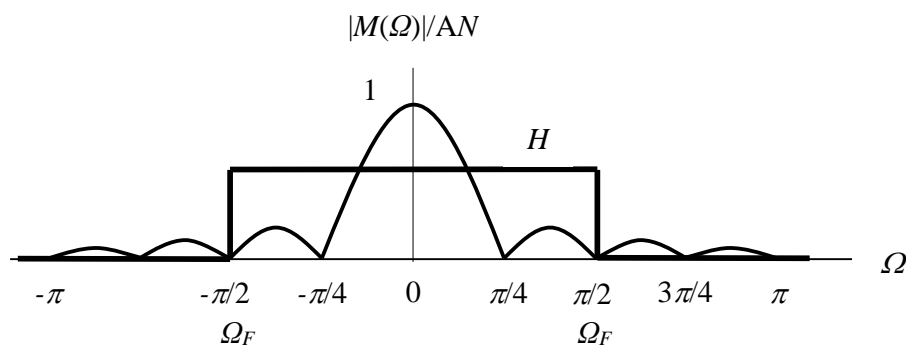


Figure 15 – Spectra of the rectangular pulse and the impulse response of the LP filter  
 Рис. 15 – Спектры прямоугольного импульса и импульсная характеристика LP-фильтра

Слика 15 – Спектар правоугаоног пулса и импулсног одзива нископропусног филтера

*LPF output signal.* The output of the filter is a bandlimited signal having the spectrum defined as

$$M_F(\Omega) = M(\Omega) \cdot H(\Omega) = \begin{cases} ANH & \Omega = 0 \\ AHe^{-j\Omega(N-1)/2} \frac{\sin(\Omega N / 2)}{\sin(\Omega / 2)} & |\Omega| \leq \Omega_F \end{cases}, \quad (44)$$

as presented in Figure 15 between the cut-off frequencies  $-\Omega_F$  and  $+\Omega_F$ .

*Analysis of the filter operation in the time domain and the frequency domain.* The filtering process is presented in the frequency domain as the multiplication of the amplitude spectral densities of the input signal  $m(n)$  and the impulse response  $h(n)$ . This multiplication in the frequency domain corresponds to the convolution of the signals in the time domain.

Therefore, the filter output signal in the time domain  $m_F(n)$  is the convolution of the filter impulse response  $h(n)$ , which is the sinc function obtained as the discrete-time inverse Fourier transform (DTIFT) of the spectrum  $H(\Omega)$ , and the input signal  $m(n)$ . The impulse response of the LP filter is calculated as

$$\begin{aligned}
 h(n) &= \frac{1}{2\pi} \int_{-\pi}^{\pi} H(\Omega) e^{+j\Omega n} d\Omega = \frac{1}{2\pi} \int_{-\Omega_F}^{\Omega_F} H e^{+j\Omega n} d\Omega = \frac{H}{2\pi} \frac{e^{+j\Omega n}}{jn} \Big|_{-\Omega_F}^{\Omega_F} \\
 &= \frac{H}{\pi n} \frac{e^{+j\Omega_F n} - e^{-j\Omega_F n}}{2j} = \frac{H\Omega_F}{\pi n\Omega_F} \sin\Omega_F n = \frac{H\Omega_F}{\pi} \text{sinc}\Omega_F n, \quad (45) \\
 &= \frac{H}{\Omega_F = \pi/2} \text{sinc}\pi n / 2
 \end{aligned}$$

having the zero crossings calculated as:  $\sin(\pi n / 2) = 0$ ,  $(\pi n / 2) = k\pi$ ,  $n = 2k$ , as shown in Figure 16.

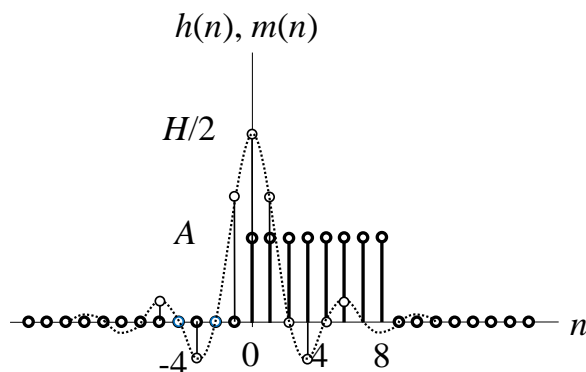


Figure 16 – Impulse response and the output of the ideal LP filter  
 Рис. 16 – Импульсная характеристика и выходной сигнал идеального LP-фильтра  
 Слика 16 – Импулсни одзив и излаз идеалног нископропусног филтера

The energy of the impulse response in the time domain can be calculated as

$$E_h = \sum_{n=-\infty}^{\infty} h^2(n) = \sum_{n=-\infty}^{\infty} \left[ \frac{H}{2} \text{sinc}\pi n / 2 \right]^2, \quad (46)$$

and in the frequency domain

$$E_H = \frac{1}{2\pi} \int_{-\pi}^{\pi} |H(\Omega)|^2 d\Omega = \frac{H^2}{2\pi} \int_{-\pi/2}^{\pi/2} d\Omega = \frac{H^2}{2}. \quad (47)$$



The filtered signal in the time domain is the convolution of the rectangular pulse  $m(n)$  and the impulse response  $h(n)$ , i.e.,

$$m_F(n) = \sum_{l=-\infty}^{l=\infty} m(n-l)h(l) = \sum_{l=-\infty}^{l=\infty} h(n-l)m(l). \quad (48)$$

This convolution can be calculated if the values of the *sinc* function are calculated and represented by a series of numbers (sufficiently long) and then convolved with the values of  $m(n)$  represented by a finite series of ones. Since the discrete-time Fourier transform of the filtered signal is

$$M_F(\Omega) = \begin{cases} ANH & \Omega = 0 \\ AH e^{-j\Omega(N-1)/2} \frac{\sin(\Omega N / 2)}{\sin(\Omega / 2)} & |\Omega| \leq \Omega_F \end{cases}, \quad (49)$$

the energy of the signal can be very accurately calculated as it has been already done in (13), i.e.,

$$E_{MF} \approx \frac{1}{2\pi} \int_{-\pi}^{\pi} |M_F(\Omega)|^2 d\Omega = \frac{A^2}{2\pi} \int_{-\pi/2}^{\pi/2} \left\| \frac{\sin(\Omega N / 2)}{\sin(\Omega / 2)} \right\|^2 d\Omega = \frac{2}{\pi} 48.295. \quad (50)$$

Having in mind that the carrier is expressed as  $s_c(n) = \cos \Omega_c n$  and that it has 4 samples per oscillation, the spectrum of the modulated signal is a shifted version of the spectrum of the filtered rectangular pulse, i.e.,

$$\begin{aligned} S_F(\Omega) &= FT\{m_F(n) \cos \Omega_c n\} = \frac{1}{2} FT\{m_F(n)(e^{j\Omega_c n} + e^{-j\Omega_c n})\} \\ &= \frac{1}{2} [M_F(\Omega - \Omega_c) + M_F(\Omega + \Omega_c)] \end{aligned} \quad (51)$$

where

$$\frac{1}{2} M_F(\Omega - \Omega_c) = \begin{cases} ANH / 2 & (\Omega - \Omega_c) = 0 \\ \frac{AH}{2} e^{-j(\Omega - \Omega_c)(N-1)/2} \frac{\sin((\Omega - \Omega_c)N / 2)}{\sin((\Omega - \Omega_c) / 2)} & |\Omega - \Omega_c| \leq \Omega_F \end{cases}, \quad (52)$$

and

$$\frac{1}{2} M_F(\Omega + \Omega_c) = \begin{cases} ANH / 2 & (\Omega + \Omega_c) = 0 \\ \frac{AH}{2} e^{-j(\Omega + \Omega_c)(N-1)/2} \frac{\sin((\Omega + \Omega_c)N / 2)}{\sin((\Omega + \Omega_c) / 2)} & |\Omega + \Omega_c| \leq \Omega_F \end{cases}, \quad (53)$$

which is presented in Figure 17.

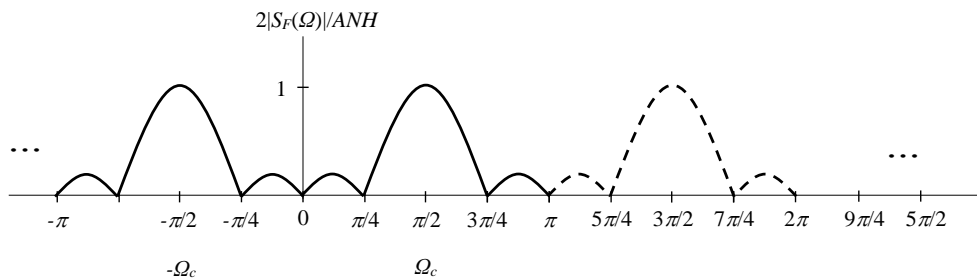


Figure 17 – Magnitude spectral density of the modulated filtered pulse  
 Рис. 17 – Спектральная плотность модулированного отфильтрованного импульса  
 Слика 17 – Спектрална густина магнитуде филтрираног модулисаног пулса

The spectrum of the modulated pulse, as a function of the angular frequency, is shown in Figure 17. The filtered modulated pulse in the time domain is a product of the filtered pulse and the carrier, i.e.,

$$s_F(n) = s_c(n) \cdot m_F(n) = \cos \pi n / 2 \cdot \sum_{l=-\infty}^{l=\infty} h(n-l)m(l) \quad (54)$$

This is the modulated signal which has a limited bandwidth. This signal is transmitted through the channel and processed in the receiver as presented in the previous sections.

## Conclusions

This paper presented a theoretical model and the simulation results of a discrete-time communication system. The block schematic of the system's transmitter and receiver is presented in the form of mathematical operators and all input-output signals are presented in both the time domain and the frequency domain. The powers and energies of the signals are calculated and the attenuation of the signals is analyzed.

Two types of transmitters are synthesized: one with an ideal rectangular discrete time pulse and one with a filtered rectangular pulse. It is shown that the application of a filter inside the transmitter reduces the modulating signal spectrum thus causing the reduction of the modulated signal bandwidth. Furthermore, two receivers are analyzed: a receiver that uses a low-pass filter for demodulation and a receiver that uses a correlator for received signal demodulation. All theoretical results are confirmed by simulations.

## References

- Abramowitz, M. & Stegun, I.A. 1972. *Handbook of Mathematical Functions with Formulas, Graphs, and Mathematical Tables*. Washington, D.C.: United States Department Of Commerce, National Bureau of Standards, Applied Mathematics Series – 55 [online]. Available at: <https://personal.math.ubc.ca/~cbm/aands/frameindex.htm> [Accessed: 20 January 2023].
- Benvenuto, N., Corvaja, R., Erseghe, T. & Laurenti, N. 2007. *Communication Systems, Fundamentals and Design Methods*. Hoboken, NJ, USA: John Wiley & Sons, Inc. ISBN-13: 978-0470018224.
- Berber, S. 2009. *Deterministic and Stochastic Signal Processing: Continuous and Discrete-time Signals*. VDM Verlag Dr. Müller. ISBN-13: 978-3639111880.
- Berber, S. 2019. Discrete time domain analysis of chaos-based wireless communication systems with imperfect sequence synchronization. *Signal Processing*, 154, pp.198-206. Available at: <https://doi.org/10.1016/j.sigpro.2018.09.010>.
- Berber, S. 2021. *Discrete Communication Systems*. Oxford, UK: Oxford University Press. ISBN-13: 978-0198860792.
- Cavicchi, T.J. 2000. *Digital Signal Processing, Solutions Manual*. Hoboken, NJ, USA: John Wiley & Sons, Inc. [Accessed: 20 January 2023].
- Haykin, S. 2001. *Digital Communication Systems, 4th edition*. Hoboken, NJ, USA: John Wiley & Sons, Inc. ISBN: 0-471-17869-1.
- Ingle, V.K. & Proakis, J.G. 2012. *Digital signal processing using MATLAB, 3rd edition*. Stamford, CNT, USA: Cengage Learning. ISBN-13: 978-1-111-42737-5.
- Integral calculator. 2023. *Calculate integrals online – with steps and graphing!* [online]. Available at: <https://www.integral-calculator.com> [Accessed: 20 January 2023].
- Manolakis, D.G., Ingle, V.K. & Kogan, S.M. 2005. *Statistical and Adaptive Signal Processing: Spectral Estimation, Signal Modeling, Adaptive Filtering and Array Processing, Illustrated edition*. Norwood, MA, USA: Artech House. ISBN-13: 978-1580536103.
- Miao, G.J. 2007. *Signal Processing in Digital Communications*. Norwood, MA, USA: Artech House. ISBN 13: 978-1-58053-667-7.
- Papoulis, A. & Pillai, S.U. 2002. *Probability, Random Variables, and Stochastic Processes, 4th edition*. McGraw-Hill Europe. ISBN-13: 978-0071226615.
- Proakis, J.G. 2001. *Digital Communications, 4th edition*. McGraw Hill Higher Education. ISBN-13: 978-0071181839.
- Quyen, N.X., Yem, V.V. & Duong, T.Q. 2015. Design and analysis of a spread-spectrum communication system with chaos-based variation of both phase-coded carrier and spreading factor. *IET Communications*, 9(12), pp.1466-1473. Available at: <https://doi.org/10.1049/iet-com.2014.0907>.
- Rice M. 2009. *Digital Communications: A Discrete-time Approach, 1st edition*. London, UK: Pearson Prentice Hall. ISBN-13: 978-0130304971.

Математическое моделирование и имитация передатчика  
прямоугольных импульсов в дискретном времени

Стеван М. Бербер

Университет Окленда,  
Кафедра электротехники, вычислительной техники и программного  
обеспечения, г. Окленд, Новая Зеландия

РУБРИКА ГРНТИ: 50.07.03 Теория и моделирование вычислительных  
сред, систем, комплексов и сетей

ВИД СТАТЬИ: оригинальная научная статья

**Резюме:**

*Введение/цель:* В данной статье обсуждаются вопросы теории и разработки системы связи в дискретном времени, используемой для передачи импульсов дискретного времени с фильтрацией и без нее. Сигналы анализируются как во временной, так и в частотной областях.

*Методы:* Система теоретически проанализирована на основе блок-схемы, которая была представлена в виде математических операторов, по которым выполнено моделирование системы для подтверждения теоретических выводов.

*Результаты:* Сигналы дискретного времени представлены во временной и частотной областях, и подтверждены методом имитационного моделирования, разработанного в Matlab.

*Выводы:* Результаты данного исследования вносят вклад в теоретическое моделирование и разработку современных дискретных систем связи.

*Ключевые слова:* дискретная система связи, разработка системы, передатчик дискретных импульсов, фильтрация, корреляционный приемник.

---

Математичко моделовање и симулација примопредајника  
правоугаоних импулса за рад у дискретном времену

Стеван М. Бербер

Универзитет у Окланду,  
Катедра за електротехнику, рачунарску и софтверску технику,  
Окленд, Нови Зеланд

ОБЛАСТ: телекомуникације  
КАТЕГОРИЈА (ТИП) ЧЛАНКА: оригинални научни рад

**Сажетак:**

*Увод/циљ:* У раду су приказани теорија и дизајн телекомуникационог  
суistema који ради у дискретном времену. Он се користи за пренос

*филтрираног и нефилтрираног дискретног пулса. Сигнали су анализирани у временском и фреквенцијском домену.*

*Методe: Систем је теоријски анализиран на основу блок-шеме која је приказана у форми математичких оператора, према којој је извршена и симулација система како би се потврдили теоријски налази.*

*Резултати: Сигнали дискретног времена презентирани су у временском и фреквенцијском домену и потврђени симулацијом у Матлабу.*

*Закључак: Резултати овог рада доприносе теоријском моделовању и дизајну модерних дискретних комуникационих система.*

*Кључне речи: дискретни комуникациони систем, дизајн система, примопредајник дискретног пулса, филтрирање, корелациони пријемник.*

Paper received on / Дата получения работы / Датум пријема чланка: 24.01.2023.

Manuscript corrections submitted on / Дата получения исправленной версии работы / Датум достављања исправки рукописа: 25.03.2023.

Paper accepted for publishing on / Дата окончательного согласования работы / Датум коначног прихватања чланка за објављивање: 27.03.2023.

© 2023 The Author. Published by Vojnotehnički glasnik / Military Technical Courier (www.vtg.mod.gov.rs, втг.мо.упр.срб). This article is an open access article distributed under the terms and conditions of the Creative Commons Attribution license (<http://creativecommons.org/licenses/by/3.0/rs/>).

© 2023 Автор. Опубликовано в «Военно-технический вестник / Vojnotehnički glasnik / Military Technical Courier» (www.vtg.mod.gov.rs, втг.мо.упр.срб). Данная статья в открытом доступе и распространяется в соответствии с лицензией «Creative Commons» (<http://creativecommons.org/licenses/by/3.0/rs/>).

© 2023 Аутор. Објавио Војнотехнички гласник / Vojnotehnički glasnik / Military Technical Courier (www.vtg.mod.gov.rs, втг.мо.упр.срб). Ово је чланак отвореног приступа и дистрибуира се у складу са Creative Commons лиценцом (<http://creativecommons.org/licenses/by/3.0/rs/>).

